



Structural studies of sub monolayer Sn/Cu(001) structures

J. Lallo^a, L.V. Goncharova^a, B.J. Hinch^{a,*}, S. Rangan^b, R.A. Bartynski^b, D.R. Strongin^c

^a Department of Chemistry and Chemical Biology, Laboratory of Surface Modification, Rutgers University, NJ 08854, United States

^b Department of Physics and Astronomy, Laboratory of Surface Modification, Rutgers University, NJ 08854, United States

^c Department of Chemistry, Temple University, Philadelphia, PA 19122, United States

ARTICLE INFO

Article history:

Received 28 November 2007

Accepted for publication 22 April 2008

Available online 7 May 2008

Keywords:

Atom-solid scattering and diffraction-elastic

Scanning tunneling microscopy

Surface relaxation and reconstruction

Surface stress

Surface structure, morphology, roughness,
and topography

Copper

Tin

Adatoms

ABSTRACT

Helium atom scattering (HAS) and scanning tunneling microscopy (STM) have been used to investigate five ordered phases formed by Sn-evaporation and deposition on room temperature Cu(001) surfaces. Complementary Auger (AES) and electron diffraction (LEED) studies have also been performed. Glide plane symmetry has been noted in a $p(2 \times 6)$ phase. The $c(4 \times 8)$, $p(3\sqrt{2} \times \sqrt{2})$, and $c(4 \times 4)$ phases exhibit measurable lateral relaxations. The $c(4 \times 8)$ and $c(4 \times 4)$ phases have Sn in distorted nearest-neighbor adsorption sites. New structural models are proposed for four Sn/Cu phases. Each of these models is discussed in light of the lateral stress relief mechanisms that are operative. STM topographic details are used to argue in favor of the prevalence of 2-D alloy-like structures in most phases. We speculate also on the necessity of subsurface vacancies in formation of the $p2mg$, $p(2 \times 6)$ ordered phase.

© 2008 Elsevier B.V. All rights reserved.

1. Introduction

The ordering of metallic adsorbates on copper surfaces has been subject to much study [1–3]. In part because of the well known 3-D bronze alloy, the structure and properties of tin films on copper surfaces have been extensively investigated, both in submonolayer [4–8] and multilayer [9,10] coverage regimes. The large lattice mismatch between tin and copper contributes to a complex yet well defined series of ordered phases formed with room temperature Sn exposure of Cu(001). (a_{Sn} is $\sim 10\%$ greater than a_{Cu} .) LEED studies [4,11] of the Sn/Cu(001) system have identified five room temperature Sn super-structures; i.e. the “ $p(2 \times 2)$ ”, $p(2 \times 6)$, $c(4 \times 8)$, $p(3\sqrt{2} \times \sqrt{2})$ and $c(4 \times 4)$ phases. These were observed between 0.24 ML and 0.7 ML coverages of Sn. No ordered structures have been reported with room temperature Sn levels in excess of 0.7 ML. In contrast to Sn on Cu(001), Sn on Cu(111) does not exhibit such a rich phase diagram [6].

Both helium atom scattering [12] (HAS) and scanning tunneling microscopy [13] (STM) have been used to study similar bi-metallic systems. This paper concentrates explicitly on the interpretation of these techniques' observations from the ordered Sn/Cu(001) phases. We report here a new symmetry requirement for the $p(2 \times 6)$ phase and the first real-space images of the $c(4 \times 8)$,

$p(3\sqrt{2} \times \sqrt{2})$ and $c(4 \times 4)$ phases. This new information places additional constraints on the overlayer structure models and we suggest new models for some phases.

It has been reported that 2-D alloying occurs for at least some of the sub monolayer coverage Sn/Cu(001) phases [14]. In simple substitutional surface alloy formation, lateral stress levels must grow as the Sn densities increase [15]. Consequently, all alloy superstructures will exhibit means for stress relief within these phases. In this paper we raise the possibility of another distinct means, to be added to the commonly accepted catalog of possible lateral stress relief mechanisms, that may be active in the Sn/Cu(001) system. Finally, based on the argument that increasing in-plane vacancy densities must increase monotonically with Sn density, we are able to arrive at one sequence of models that is consistent with all observations, and thus represents our best assignments for the structure of each room temperature Sn/Cu(001) phase. We suggest that the approach used here may be applicable also to other alloying systems which exhibit rich phase diagrams.

2. Experimental

Two ultra-high vacuum chambers were used to obtain the results presented in this work. LEED, AES, and high-resolution HAS studies were conducted in the first system, and STM, LEED and

* Corresponding author. Tel.: +1 732 445 0663.

E-mail address: jhinch@rutchem.rutgers.edu (B.J. Hinch).

AES data were acquired in a second system. Both UHV chambers had base pressures of below 2×10^{-10} Torr.

In both systems, Cu(001) crystals were cleaned by 30 minute cycles of 600 eV Ar⁺ sputtering followed by 850K annealing. A higher sputtering voltage (1500 V) was often needed to remove the residual surface tin atoms. After sputter cleaning, no surface tin, oxygen or carbon contaminants were observed, as measured by Auger spectroscopy.

In the first system, which has been described in detail elsewhere, [16] tin deposition was first monitored in helium atom specular, $\Theta_i = \Theta_f = 49.5^\circ$, reflectivity measurements, over a range of substrate temperatures. A maximum in helium atom reflectivity curves was ascribed to the completion of the $p(3\sqrt{2} \times \sqrt{2})$ phase at a Sn coverage of 0.5 ML, and all coverages were referenced to this coverage. (All of our data is consistent with this assertion.) The Sn deposition was also monitored with a quartz crystal microbalance, and Auger measurements were taken with a PHI double pass cylindrical mirror analyzer. Auger spectra were recorded after each deposition and ratios, between the Sn(MNN) and Cu(LMM) peak features at 430 eV and 920 eV, respectively, were used for relative coverage determination. The Auger feature ratio was used also for direct comparison with measurements taken in the second UHV system. The Auger ratio was found to be proportional to the Sn coverage, for all but the $c(4 \times 4)$ phase. This highest coverage phase exhibited a slightly enhanced Sn to Cu Auger ratio.

The second system consists of a UHV Omicron VT Scanning Probe Microscope connected with UHV sample transfer to a sample preparation/analysis chamber. The latter chamber includes LEED, Auger, sputtering ion gun, and metal evaporation sources. The same Sn-evaporation source from the HAS measurements was used in this chamber, and Sn deposition was monitored by a quartz crystal monitor (QCM). The Sn coverages were calibrated by using Auger peak intensity ratios as in the other system. LEED was used to confirm surface structure formation. All STM measurements were performed at room temperature and, in contrast to step-edge images which were seen for a wide range of tunneling conditions, Sn structures were reproducibly observed only in a narrow range of low voltage and high current conditions. All STM images shown in this paper were taken at $\sim +5$ mV tip bias and ~ 7 nA tunnel current and in a constant current tunneling mode.

3. Results and discussion

He atom specular reflectivity was monitored during Sn uptake. For samples at room temperature, the complex structure of these curves, such as shown in Fig. 1(a), is indicative of a sequence of ordering phenomena. Local intensity maxima are indicators of completion, or near completion, of ordered phases. Sequential He diffraction scans show many of these phases can coexist, but the following order of phases with increasing Sn coverage is adhered to: what we refer to as “ $p(2 \times 2)$ ”, $p(2 \times 6)$, $c(4 \times 8)$, $p(3\sqrt{2} \times \sqrt{2})$ and $c(4 \times 4)$ phases, respectively. At least one report of studies on each of these phases is found in the literature.

The uptake curves in specular reflectivity vary slightly with uptake rate. For example, we have observed that the relative specular intensity of the $p(3\sqrt{2} \times \sqrt{2})$ phase is almost tripled if the Sn deposition rate is reduced to ~ 0.016 ML/min. Kinetic limitations in surface restructuring are implied, particularly of this 0.5 ML phase. The shape of the uptake curve also has a dependence on the scattering azimuth. This is a non kinematic effect, implying the significance of He multiple scattering in scattered intensities from at least some of the ordered phases.

Although we report evidence for kinetic effects in phase formation, we have found no direct evidence for simultaneous coexis-

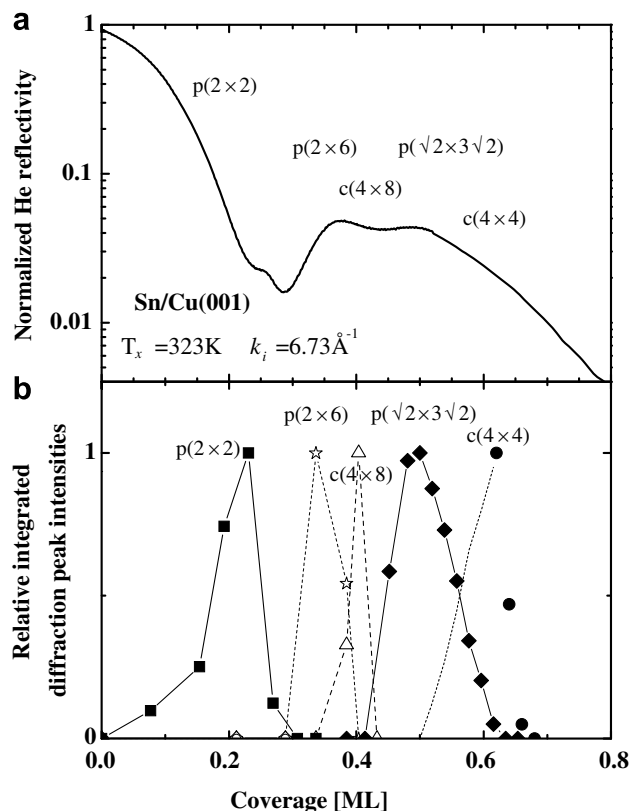


Fig. 1. He diffraction intensities scattered from Cu(001) at 300 K, and at varying Sn coverages. (a) He specular reflectivities normalized to that of the clean surface. The scattering geometry was aligned along the $[1\bar{1}0]$ azimuth. Total uptake curve duration shown, 5 min. (b) Integrated diffraction peak intensities, using diffraction peaks of identified phases taken along both $[100]$ and $[1\bar{1}0]$ azimuths using $E_i = 23.65$ meV, $k_i = 6.73 \text{ \AA}^{-1}$. Discrete peaks used are listed in the text. Integrated intensities are approximated by $\sum_{\text{peaks}} I \cdot \text{FWHM}^2$. With the exception of the $c(4 \times 4)$ phase (see text), the “integrated intensities” are then normalized to their maximum value (for each phase.) In both (a) and (b) cumulative coverages are scaled such that the $p(\sqrt{2} \times 3\sqrt{2})$ phase is maximized at 0.5 ML of Sn.

tence of three or more ordered phases on the surface. The coexistence of only two ordered phases at any time is fully consistent with diffraction intensity observations. Normalized integrated diffraction peak intensities are shown in Fig. 1(b), and were determined using the following diffraction peaks; the split diffraction maxima at $\sim (1/2, 1/2)$ for the “ $p(2 \times 2)$ ” phase: $(1/3, 0)$ and $(2/3, 0)$ for $p(2 \times 6)$: $(1/4, 0)$ and $(3/4, 0)$ for $c(4 \times 8)$: $(2/6, 2/6)$ and $(5/6, 5/6)$ only for $p(3\sqrt{2} \times \sqrt{2})$. For the $c(4 \times 4)$ phase the $(1/2, 1/2)$ peak intensity is used only after complete loss of the $p(3\sqrt{2} \times \sqrt{2})$ phase.

Unlike the other preceding lower coverage phases, it is not certain if the $c(4 \times 4)$ phase can be formed in the absence of a coexisting phase. Below 0.625 ML some $p(3\sqrt{2} \times \sqrt{2})$ phase is always present. At higher coverages the integrated peak intensities decrease immediately, suggesting increased disorder and formation of a presumed multilayer phase (without measurable diffraction peak intensities). At a Sn coverage of ~ 0.7 ML even the specular feature is almost absent. Thus, we cannot be certain that the $c(4 \times 4)$ phase can fill the entire surface. Therefore, in Fig. 1(b), the points of the $c(4 \times 4)$ phase use a different means of normalization. Generally, the normalized integrated diffraction peak intensities are meant to be suggestive of fractional surface areas coverage, of each phase. The sum of fractional areas, at any coverage, should not exceed one. Consequently, for the $c(4 \times 4)$ phase, the dashed line rising from 0.5 ML to 0.61 ML is simply a curve given by $1-x$, where x = the values for the $p(3\sqrt{2} \times \sqrt{2})$ phase,

Download English Version:

<https://daneshyari.com/en/article/5425068>

Download Persian Version:

<https://daneshyari.com/article/5425068>

[Daneshyari.com](https://daneshyari.com)